Cancer Letters 461 (2019) 1–9

Contents lists available at ScienceDirect

Cancer Letters

journal homepage: www.elsevier.com/locate/canlet

Original Articles

Improved anti-tumor efficacy of paclitaxel in combination with MicroRNA-125b-based tumor-associated macrophage repolarization in epithelial ovarian cancer

Neha N. Parayath[a,1], Srujan Kumar Gandham[a], Fraser Leslie[a], Mansoor M. Amiji[a,b,*]

[a] Department of Pharmaceutical Sciences, School of Pharmacy, Boston, MA, 02115, USA
[b] Department of Chemical Engineering, College of Engineering, Northeastern University, Boston, MA, 02115, USA

ARTICLE INFO

Keywords:
Hyaluronic acid-poly(ethylene imine) nanoparticles
Chemotherapy
ID8-VEGF ovarian cancer model
Intraperitoneal chemotherapy
Immune-suppressive macrophages

ABSTRACT

In epithelial ovarian cancers, the presence of tumor-associated macrophages (TAMs) is well correlated with the poor disease outcomes. TAMs are know to suppress the immune system, induce pro-tumoral functions and inhibit anti-tumor responses associated with chemotherapy. In this study, we have evaluated the synergistic efficacy of TAM repolarization and intraperitoneal paclitaxel in epithelial ovarian cancers. We demonstrate that hyaluronic acid-based nanoparticles encapsulating miR-125b (HA-PEI-miR-125b) can specifically target TAMs in the peritoneal cavity of a syngeneic ID8-VEGF ovarian cancer mouse model and can repolarize macrophages to an immune-activating phenotype. These HA-PEI-miR-125b nanoparticles in combination with intraperitoneal paclitaxel can enhance the anti-tumor efficacy of paclitaxel during the later stages of disease progression as seen by the significant reduction in the ascitic fluid and peritoneal VEGF levels. Furthermore, these HA-PEI-miR-125b nanoparticles do not induce systemic toxicity and thus warrant a further evaluation in the clinical setting.

1. Introduction

Ovarian cancer is the fifth leading cause of cancer-related deaths among women in the United States [1]. According to the American Cancer Society, more than 22,240 women received a new diagnosis of ovarian cancer and about 14,070 women succumbed from the disease in 2018 [2]. The vast majority of the cases of ovarian cancer originate from epithelial cells in the ovaries. Early-stage epithelial ovarian cancer is generally asymptomatic [3], where 75% of ovarian cancer cases are diagnosed as a late-stage disease [4]. Ovarian cancer management consists of primary cytoreductive surgery followed by paclitaxel-platinum combination chemotherapy [5]. Though the response rate to paclitaxel-platinum is about 80%, the major issue of concern is disease recurrence [6]. Among women with advanced ovarian cancer, about 50–75% demonstrate relapse [7]. With the current advances in understanding the immune component of ovarian cancers, there is a unique opportunity to develop clinically translatable combination treatment modalities that are expected to improve outcomes among advanced refractory patients.

The heterogeneous microenvironment of ovarian tumors contains cancer cells, stromal cells, and immune cells which co-exist in a dynamic state. The tumor-associated macrophages (TAMs), which represent about 50% of the solid tumor mass in certain adavanced staged cancers, are primarily of the anti-inflammatory (or alternatively activated M2) phenotype; these TAMs foster tumor development by inducing immune suppression, angiogenesis, and metastasis [8–10]. TAMs are derived from circulating monocytic precursors and recruited to the tumor site by cytokines, chemokines, and other tumor-derived factors. Studies have shown that colony-stimulating factor-1 (CSF-1) derived from ovarian tumor tissue induces macrophages to polarize toward the anti-inflammatory phenotype, in turn promoting tumor growth [11]. In epithelial ovarian cancers, the number of macrophages and amount of CSF-1 increase with disease progression [12]. In relapse-free survival patients, the levels of the anti-inflammatory macrophage marker CD163 on TAMs is inversely correlated with immunosuppressive cytokine levels in ascitic fluid [13]. Repolarization of TAMs from an anti-inflammatory to a pro-inflammatory phenotype could aid in disease regregression and enhance the anti-tumor efficacy of therapeutics in ovarian cancer. Various strategies such as the use of small molecules, interferons, and interleukins have demonstrated successful repolarization of TAMs [14–18] and are being evaluated in clinical trials [19]. However, the major limitation associated with repolarization strategies

* Corresponding author. Department of Pharmaceutical Sciences, School of Pharmacy, Boston, MA, 02115, USA.
E-mail address: m.amiji@northeastern.edu (M.M. Amiji).
[1] Current address: Clinical Research Division, Fred Hutchinson Cancer Research Center, Seattle, WA, 98,109, USA.

https://doi.org/10.1016/j.canlet.2019.07.002
Received 11 January 2019; Received in revised form 28 June 2019; Accepted 2 July 2019

has been the inability to selectively target macrophages.

The TAMs are known to express a variety of pathologically relevant miRs. These miRs can affect the phenotype exhibited by TAMs; hence, the molecular mechanisms underlying TAM polarization by miRs has been an area of intense investigation. In particular, miR-125b is expressed at higher levels in macrophages than in other immune cells and has been shown to regulate macrophage activation [20]. We have previously shown that selective macrophage transfection with miR-125b using hyaluronic acid-poly(ethyleneimine) (HA-PEI) nanoparticles led to > 6-fold increase in the M1 to M2 macrophage ratio and 300-fold increase in the iNOS (M1 marker)/Arg-1 (M2 marker) ratio as compared to the untreated control group in lung tissues from a non-small cell lung cancer mouse model [21]. Additionally, studies have demonstrated the role of repolarization of TAMs as an immunotherapy and have proposed that repolarization of TAMs could complement other forms of anti-cancer therapy [22]. Given this, we have evaluated the synergistic anti-tumor efficacy of repolarization of TAMs using HA-PEI-miR-125b nanoparticles, in combination with paclitaxel therapy for the treatment of epithelial ovarian cancer.

2. Materials and methods

2.1. Materials

Sodium hyaluronate (HA) 20–40K was purchased from Lifecore Biomedical Co. (Chaska, MN). *N*-(3-dimethylaminopropyl)-N′-ethyl-carbodiimide hydrochloride (EDC), *N*-hydroxysuccinimide (NHS), poly (acrylic acid) (PAA) and RPMI-1640 media were purchased from Sigma-Aldrich Chemical Co. (St. Louis, MO, USA). Branched poly (ethyleneimine) (bPEI) 10,000 Da was purchased from Polysciences Inc. (Warrington, PA). Dialysis membrane of 12–14 kDa molecular weight cut-off (MWCO) was obtained from Spectrum Laboratories Inc., CA. Cy5-NHS ester was obtained from Lumiprobe (Hallandale Beach, FL). 4% E-Gel® EX agarose gels were purchased from Thermo Scientific, PA. Fetal bovine serum (FBS) was obtained from HyClone (Logan, UT). MACS Cell Separation kit was purchased from Miltenyi Biotec, San Diego, CA. miR-125b mimic, miR-negative control and penicillin/streptomycin antibiotics were purchased from Life Technologies (Woburn, MA). Antibodies CD45, F4/80, CD11b, CD11c, PD-1, PD-L1, CD80 and CD206 antibodies were obtained from BioLegend (San Diego, CA). Primers specific for iNOS-2, Arg-1, and β-actin were purchased from Eurofins MWG Operon (Huntsville, AL).

2.2. Synthesis and characterization of HA-PEI nanoparticles

HA-PEI-miR-125b nanoparticles were synthesized as described in Ref. [21]. Briefly, HA (100 mg) was modified by a coupling reaction with PEI (15 mg) using EDC (50 mg) and NHS (50 mg) and then miR-125b was added to the HA-PEI polymer (1:27 wt ratio) to form HA-PEI-miR-125b nanoparticles. The percent encapsulation was checked using RiboGreen® assay kit as per manufactures instructions. The particle size, size distribution, zeta-potential and morphology of HA-PEI-miR-125b nano-formulations were measured using DLS (Malvern Zetasizer Nano-S, Malvern Inc., UK)and imaged by transmission electron microscopy (TEM) using uranyl acetate as described previously [21]. A gel retardation assay was carried out to analyze the release of miR-125b or scrambled miR from the HA-PEI nanoparticles using a 2% polyacrylic acid (PAA).

2.3. ID8-VEGF cell culture

ID8-VEGF epithelial ovarian cancer cells were obtained from Dr. Michael Goldberg at the Dana Farber Cancer Center (Boston, MA). ID8-VEGF cells were maintained in RPMI supplemented with 10% FBS, 5% P/S, 1% L-Glutamine, 0.5% Sodium Pyruvate and beta-ME (3.4 μl in 1000 ml medium) in 5% CO_2 at 37 °C.

2.4. ID8-VEGF syngeneic orthotopic ovarian cancer model

The animal experiments performed in this study were approved by Northeastern University's Institutional Animal Care and Use Committee. Female C57BL/6 mice (8–10 weeks old) were purchased from Charles River Laboratories (Wilmington, MA) and allowed to acclimate for 48 h prior to any procedures. Anesthesized animals were inoculated with 4 million ID8-VEGF cells through intraperitoneal injection. Post 8, 16 and 24 days, peritoneal lavage was performed with 3 ml of 1X ice-cold PBS. The cell pellets obtained after centrifugation at 400*g* for 5 min were suspended in DMEM containing 10% FBS and 1% antibiotics, were washed with PBS, and cells were then fixed with 4% paraformaldehyde and stained with macrophage markers for FACS analysis using Multi-Laser Flow Cytometry (DXP11analyzer (Cytek, Fremont, CA). The supernatant from the above peritoneal lavage was used for quantifying VEGF levels using Mouse VEGF Quantikine ELISA Kit (R&D Systems, Minneapolis, MN). Additionally, the peritoneal cavity was opened to observe the presence of tumor nodules.

2.5. Macrophage uptake of HA-PEI nanoparticles upon i.p. administration in ID8-VEGF tumor model

Female C57BL/6 mice (8–10 weeks old) were inoculated with 4 million ID8-VEGF cells through intraperitoneal injection. On the 10th-day post-tumor-cells inoculation, Cy5 labeled HA-PEI nanoparticles in PBS (0.5 mL of 1 mg/mL) was injected intraperitoneally. At 6 h, 12 h and 24 h post-injection of the HA-PEI-Cy5, the mice were sacrificed for macrophage collection from the mouse peritoneal cavity using cold PBS. The cell pellets obtained after centrifugation at 2000 rpm for 5 min were suspended in DMEM containing 10% FBS and 1% antibiotics and cultured either on coverslips or in a 6 well plate for 2 h at 37 °C with 5% CO_2. The non-adherent cells were removed by washing three times with PBS. Peritoneal macrophages on coverslips were then fixed with 4% PFA for 10 min at RT, followed by staining with Alexa flour 488-anti-mouse F4/80 antibody (a specific marker for mouse macrophages) at RT for 1 h. The coverslips were then mounted on the slide with mounting media containing DAPI and imaged under a Zeiss confocal microscope (Carl Zeiss, Cambridge, UK) at an excitation wavelength of 488 nm for F4/80 antibody and 647 nm for Cy5 labeled HA-PEI nanoparticles. The cells in the 6-well plate were treated with trypsin, fixed with 4% PFA for 10 min at RT and then stained with Alexa flour 488-anti-mouseF4/80 antibody and PE-anti-mouse CD11b antibody for FACS analysis using Mult-Laser Flow Cytometry (DXP11 Analyzer).

2.6. miR-125b transfection and TAM repolarization with HA-PEI nanoparticles

Ten days post tumor cell inoculation, the C57BL/6 mice were injected intraperitoneally with the first dose of HA-PEI-miR-125b (1 mg/kg) or HA-PEI-miR-negative control (1 mg/kg) (day 10). The second and third dose of HA-PEI-miR-125b (1 mg/kg) or HA-PEI-miR- negative control (1 mg/kg) was administered on day 12 and 14, respectively. On day 16, the mice were euthanized and peritoneal lavage was performed using cold PBS. FACS analysis was performed as described above. To obtain the peritoneal macrophages from the peritoneal exudate cells, magnetic beads conjugated to anti-mouse F4/80 antibody was used along with the MACS Cell Separation kit (Miltenyi Biotec, San Diego, CA) according to the manufacturers protocol.

The purified $F4/80^+$ peritoneal macrophages were then lysed and RNA was isolated using a High Pure RNA isolation kit from Roche Applied Sc. (Indianapolis, IN). Expression levels of iNOS and Arg-1 genes were analyzed using qPCR (LightCycler 480, Roche, Branford, CT). β -actin was used as a house-keeping gene.

2.7. Combination TAM repolarization and paclitaxel chemotherapy

Eight days post tumor cell inoculation, the C57BL/6 mice were injected intraperitoneally with a single PTX (20 mg/kg) administration, followed by HA-PEI-miR-125b (1 mg/kg) or HA-PEI-miR-negative control (1 mg/kg) on day 10, 12 and 14. On day 16, the mice were euthanized and peritoneal lavage was performed using cold PBS. FACS analysis and VEGF quantification were performed as above. Additionally, the peritoneal cavity was opened to observe the presence of tumor nodules.

2.8. Statistical data analysis

All statistical analysis was performed using Prism 6.0 software (Graph Pad Software, San Diego, CA). Results were expressed as mean ± SD. Data were analyzed using a one-way analysis of variance followed by post hoc analysis for multiple comparisons for all statistical analysis. Differences were considered statistically significant at $p < 0.05$.

3. Results

3.1. ID8-VEGF tumor model development and progression

The first segment of the study was to evaluate the syngeneic ID8 ovarian tumor model, mainly with respect to the presence of tumor-associated macrophages (TAMs) during the development and progression of these tumors. As seen in Fig. 1A the ascitic fluid starts accumulating in the peritoneal cavity by 16th day after tumor inoculation. Tumor nodules are visible on the peritoneal tissue and diaphragm on the 24th-day post tumor (Fig. 1B). The presence of TAMs ($F4/80^+$, $CD206^+$) is observed in the peritoneal cavity from 8 days post tumor inoculation and their number increases with tumor-progression at 16 days post tumor inoculation (Fig. 1C). There is a 4-fold increase in the percent of TAMs by 16 days post tumor inoculation (Fig. 1D). Additionally, since these ID8 tumor cells are VEGF expressing cells, we determined the VEGF levels in the peritoneal cavity using an ELISA-based method. The VEGF levels significantly increased, from day 8 to day 24 post tumor inoculation as compared to the control mice without tumor cell inoculation as determined by ELISA. There is a > 10-fold increase in the VEGF levels from day 8 to day 24 post tumor inoculation (Fig. 1E), thus confirming that VEGF levels could be used a marker for determining tumor progression in this syngeneic ID8 ovarian tumor model.

3.2. Synthesis and characterization of HA-PEI nanoparticles

HA-PEI nanoparticles synthesized were uniform in size as seen in the TEM image (Supplementary Fig. 1A). The HA-PEI nanoparticles with miR-125b had a size of 175.6 ± 10 nm and the HA-PEI nanoparticles with scrambled miR had a size of 169.2 ± 8 nm (Supplementary Fig. 1B). Additionally, in agreement with the TEM image, the HA-PEI nanoformulations showed a uniform size distribution with a polydispersity index (PDI) of < 0.3 (Supplementary Fig. 1B). The HA-PEI nanoformulations with miR-125b and scrambled miR showed a slight negative charge of −24.2 ± 5.3 and −28.1 ± 5.5 mV respectively (Supplementary Fig. 1B). The encapsulation efficiency of the miRs in the HA-PEI nanoparticles was 99%. Additionally, in the presence of poly (acrylic acid) (PAA), the encapsulated miR was released, as seen by the presence of a band at the molecular weight of miR-125b in Supplementary Fig. 1C.

3.3. Macrophage specific uptake of HA-PEI nanoparticles in the ID8 tumor model

The synthesized HA-PEI nanoparticles labeled with Cy5 showed a preferential uptake by the macrophages ($F4/80^+$ cells) when administrated intraperitoneally in the ID8 tumor-bearing mice on Day 10 from 6 h to 24 h (Fig. 2A). However, the Cy5 fluorescence decreases from 6 h to 24 h (Fig. 2B).

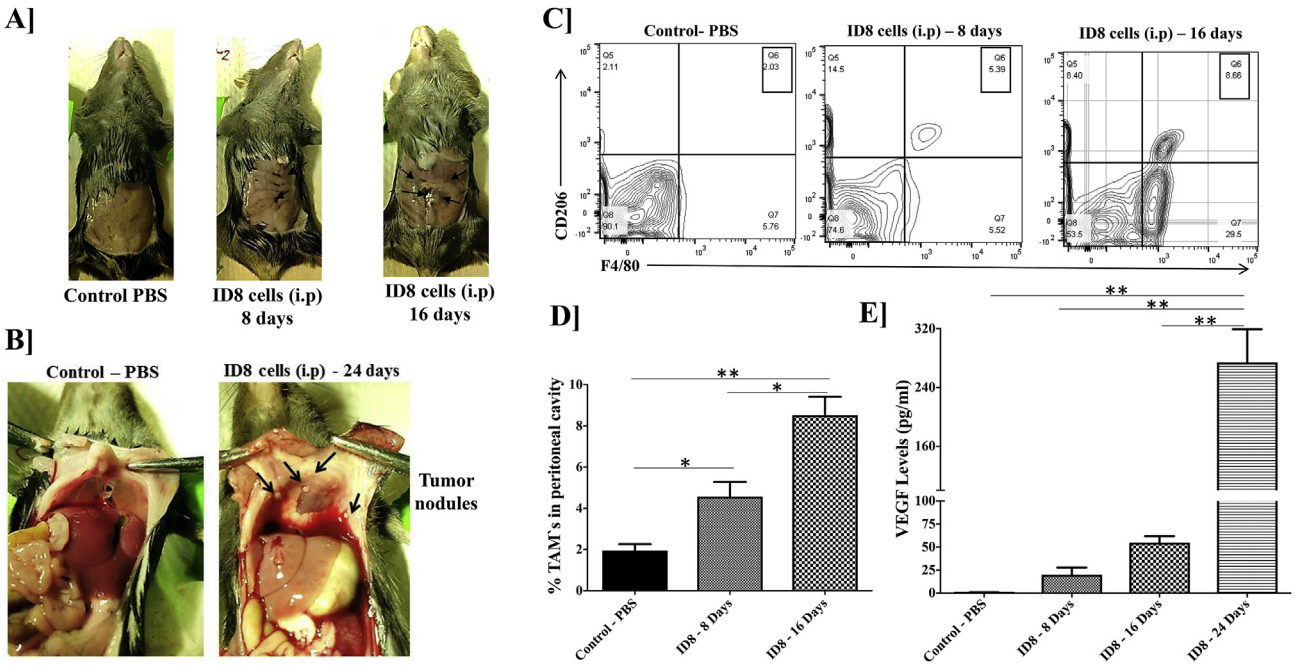

Fig. 1. ID8-VEGF epithelial ovarian tumor development in C57BL/6 mice. Female C57BL/6 mice were inoculated with 4 million ID8 cells through intraperitoneal injection. Post 8, 16 and 24 days, the peritoneal lavage was performed with 3 ml of 1X PBS. (A) Representative peritoneal cavity images from these mice. Arrows indicate accumulation of ascitic fluid. (B) The appearance of metastatic nodules on the diaphragm at Day 16. (C) FACS analysis shows the increase in TAMs with tumor progression. (E) Increase in VEGF levels in the peritoneal lavage from mice correlated with the tumor progression as determined by ELISA.

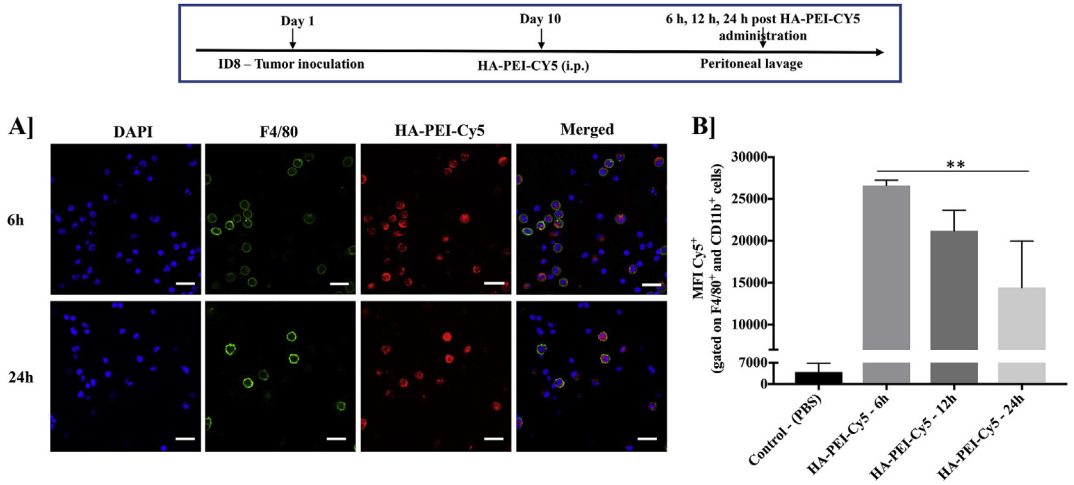

Fig. 2. Uptake of HA-PEI-Cy5 nanoparticles by macrophages in ID8 tumor-bearing mice. Female C57BL/6 mice were injected with ID8 cells on day 1. On day 10, the mice were injected intraperitoneally with Cy5 labeled HA-PEI nanoparticles and the peritoneal cavity was lavaged with 1X PBS at 6 h, 12 h, and 24 h post-administration. Representative images of cells were grown on coverslips and stained with F4/80 antibody for confocal analysis. Scale bar indicates 20 μm. (B) FACS analysis performed on the cells isolated from lavage. The graph represents MFI for Cy5 in F4/80$^+$ and CD11b$^+$ macrophages. N = 3, Data is analyzed by One-way ANOVA.

3.4. Repolarization of TAMs with miR-125b in HA-PEI nanoparticles

Intraperitoneal administration of HA-PEI nanoparticles with miR-125b or scrambled miR resulted in the reduction of total peritoneal macrophage population (CD11b$^+$, F4/80$^+$) in the ID8 ovarian tumor model as compared to the untreated control (Fig. 3A). TAMs (CD206$^+$ cells) were reduced following intraperitoneal administration of HA-PEI-miR-125b nanoparticles as compared to the untreated control (Fig. 3B). Additionally, there was > 2-fold increase in the anti-tumoral macrophages (CD80$^+$ cells), following intraperitoneal administration of HA-PEI-miR-125b nanoparticles as compared to the untreated control (Fig. 3C) and a significant reduction in the CD206/CD80 ratio with the HA-PEI-miR-125b group as compared to the untreated control (Fig. 3D). Furthermore, after isolating RNA from these macrophages, it was observed that iNOS mRNA levels were significantly increased (> 10-fold) in the HA-PEI-miR125b treatment group as compared to

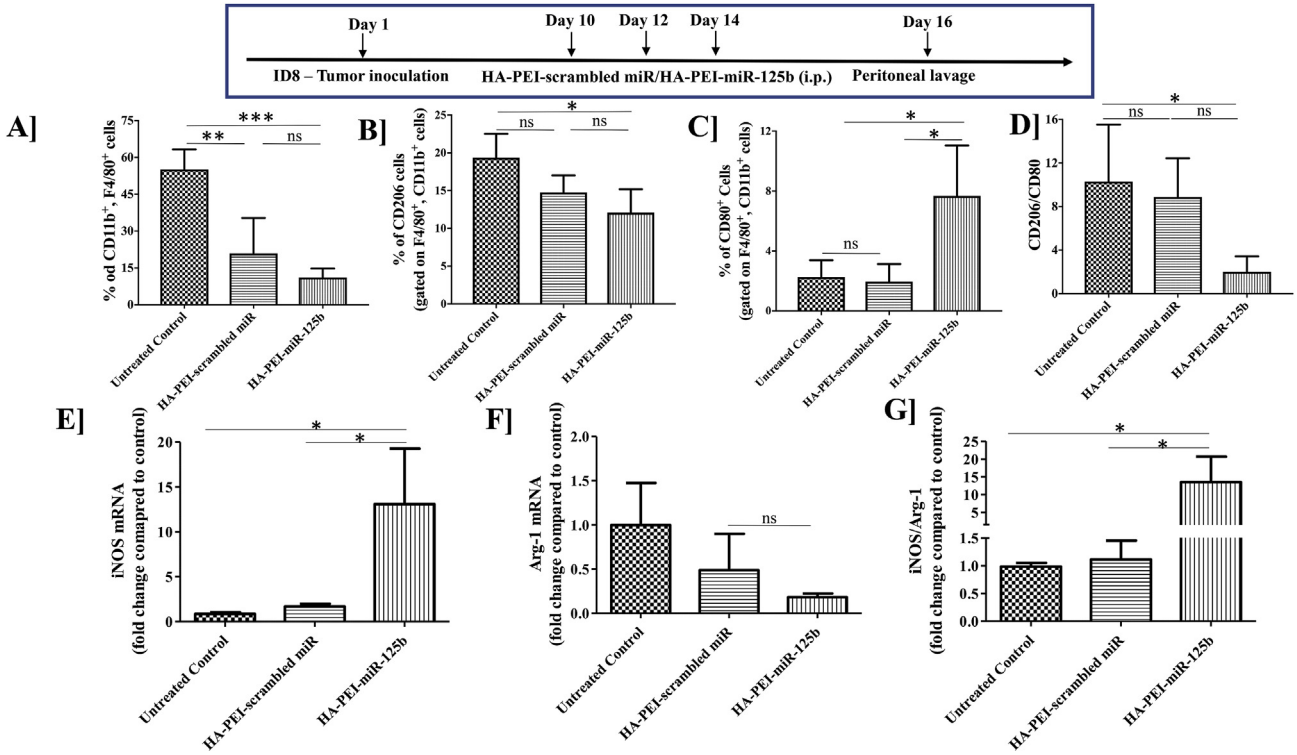

Fig. 3. Tumor-associated macrophage (TAM) repolarization using miR-125b in HA-PEI nanoparticles. Female C57BL/6 mice were injected with ID8 cells on day 1. On day 10, the mice were injected intraperitoneally with either HA-PEI-scrambled miR or HA-PEI-miR-125 b at 1 mg/kg dose every alternate day for 3 days and peritoneal cavity was lavaged with 1X PBS on day 16, for peritoneal cells collection and analysis by FACS for (A) CD11b$^+$, F4/80$^+$ macrophages, (B) CD206$^+$ M2 macrophages and (C) CD80$^+$ M1 macrophages (D) Ratio of CD206/CD80. Expression of (E) iNOS and (F) Arg-1 and (G) iNOS/Arg-1 ratio tumor-associated macrophages treated with HA-PEI nanoparticle formulations. qPCR was used for quantification of gene expression level with β-actin as the internal control. N = 4, Data is analyzed by One-way ANOVA.

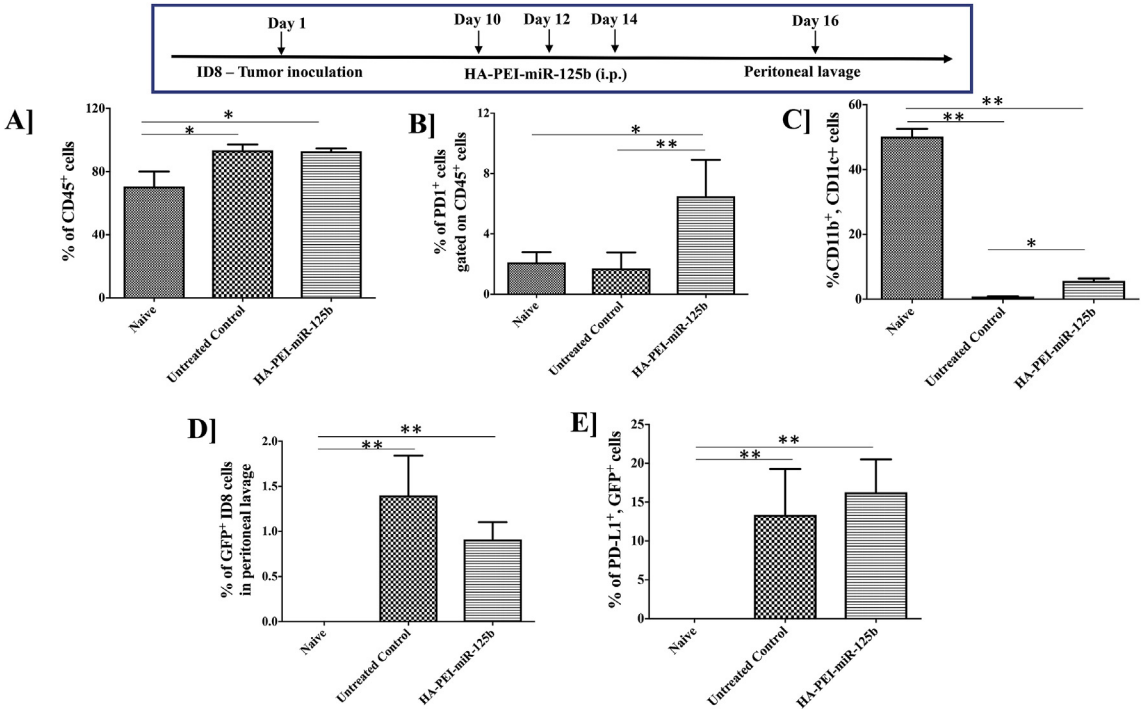

Fig. 4. Analysis of immune cells from the peritoneal lavage fluid upon miR-125b transfection. Female C57BL/6 mice were injected with ID8 cells on day 1. On day 10th mice were injected intraperitoneally with either HA-PEI-scrambled miR or HA-PEI-miR-125 b at 1 mg/kg dose every alternate day for 3 days and peritoneal cavity was lavaged with 1X PBS of day 16th for peritoneal cells collection and analysis by FACS for (A) $CD45^+$ (B) $PD1^+$ gated on $CD45^+$ cells, (C) $CD11b^+$, $CD11c^+$ dendritic cells, (D) GFP^+ ID8 cells and (E) PD-$L1^+$ with GFP^+ cells. N = 4, Data is analyzed by One-way ANOVA.

the untreated control and HA-PEI-scrambled miR groups (Fig. 3E). Additionally, the Arg-1 mRNA levels were lower in the HA-PEI-miR125b treatment group as compared to the untreated control and HA-PEI-scrambled miR groups (Fig. 3F) and the iNOS/Arg-1 mRNA ratio showed > 10-fold increase in the HA-PEI-miR125b treatment group as compared to the untreated control and HA-PEI-scrambled miR groups (Fig. 3G).

3.5. Effect of miR-125b transfection on immune cell populations

Intraperitoneal administration of HA-PEI-miR-125b nanoparticles or HA-PEI-scrambled miR, did not show any significant change in the total immune cell ($CD45^+$) population in the peritoneal cavity of tumor-bearing mice (Fig. 4A and Supplementary Fig. 2A). Interestingly, there was a significant increase in the $PD1^+$ cells following intraperitoneal administration of HA-PEI-miR-125b nanoparticles as compared to the untreated group (Fig. 4B) but no significant difference was observed in the % $PD1^+$ cells between untreated and HA-PEI-scrambled miR groups (Supplementary Fig. 2B). Additionally, there was a significant increase in the total number of dendritic cells ($CD11b^+$, $CD11c^+$) following treatment with HA-PEI-miR-125b nanoparticles and HA-PEI-scrambled miR as compared to the untreated group (Fig. 4C and Supplementary Fig. 2C). We further evaluated the effect of HA-PEI-miR-125b nanoparticles on PD-L1 levels in the tumor cells. However, there was no significant difference in the GFP^+ ID8 tumor cells and PD-$L1^+$ levels in the tumor cells following intraperitoneal administration of HA-PEI-miR-125b nanoparticles as compared to the untreated group (Fig. 4D and E and Supplementary Fig. 2E).

3.6. Effect of mir-125b-based TAM repolarization and chemotherapy combination

As seen in Fig. 5A, 24 days post tumor inoculation, following treatment with HA-PEI-miR-125b nanoparticles and paclitaxel there is a significant reduction in the ascitic fluid as compared to the untreated control, PTX treatment group, HA-PEI-miR-125b treatment group and the paclitaxel plus HA-PEI-scrambled-miR treated mice (Fig. 5A and C). There is no significant weight change observed in HA-PEI-miR-125b nanoparticles with the paclitaxel-treated group. However, the untreated control group and HA-PEI-scrambled-miR nanoparticle with paclitaxel-treated group show > 5% weight gain (Fig. 5B). Furthermore, there is a significant reduction in VEGF levels following treatment with HA-PEI-miR125b nanoparticles in combination with paclitaxel as compared to the untreated control on day 16 post tumor inoculation (Fig. 5D). On day 16th, there was no significant reduction in VEGF levels following treatment with HA-PEI-miR125b nanoparticles in combination with paclitaxel as compared to the treatment with PTX alone or HA-PEI-scrambled-miR nanoparticles in combination with paclitaxel (Fig. 5D). However, there was a significant reduction in the VEGF levels in the peritoneal lavage following treatment with HA-PEI-miR125b nanoparticles in combination with paclitaxel as compared to the treatment with PTX alone or HA-PEI-miR125b alone or HA-PEI-scrambled-miR nanoparticles in combination with paclitaxel and the untreated control on day 24 post tumor inoculation (Fig. 5D).

We also evaluated the effect of HA-PEI-scrambled-miR nanoparticle along with the paclitaxel-treated group on the tumor microenvironment. A significant reduction in the total peritoneal macrophage population ($CD11b^+$, $F4/80^+$ cells) was observed following treatment with HA-PEI-miR125b nanoparticles in combination with paclitaxel as well as treatment with HA-PEI-scrambled-miR nanoparticles in combination with paclitaxel, compared to the untreated control (Fig. 6A). There is a significant reduction in the TAM population ($CD206^+$ cells) following treatment with HA-PEI-miR125b nanoparticles in combination with paclitaxel as compared to the untreated control and treatment with HA-PEI-scrambled miR in combination with paclitaxel (Fig. 6B). Additionally, there is a significant increase in anti-tumoral macrophages ($CD80^+$ cells) following treatment with HA-PEI-miR125b nanoparticles in combination with paclitaxel as compared to the untreated control and treatment with HA-PEI-scrambled-miR nanoparticles in combination with paclitaxel (Fig. 6C). The significant reduction is

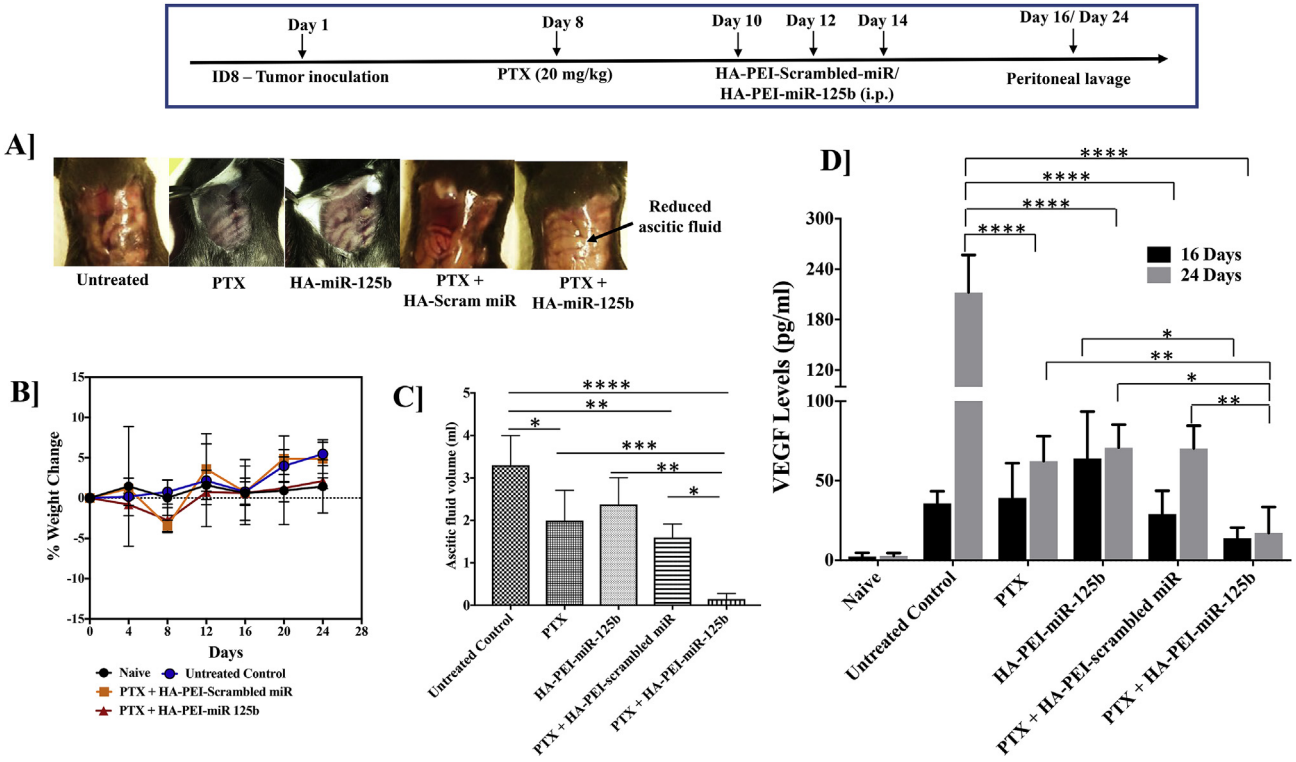

Fig. 5. Effect of combination mIR-125b transfection and paclitaxel chemotherapy on VEGF levels in the peritoneal cavity. Female C57BL/6 mice were injected with ID8 cells on day 1. On day 8th mice were injected intraperitoneally with PTX (2 mg/kg) and on day 10th mice were injected intraperitoneally with either HA-PEI-scrambled miR or HA-PEI-miR-125 b at 1 mg/kg dose every alternate day for 3 days and peritoneal cavity was lavaged with 1X PBS on Day 16 and Day 24. (A) Representative peritoneal cavity images from these mice (B) Percent change in body weight determined over the duration of the study. (C) Accumulation of ascitic fluid volume on day 24. (D) Determination of the VEGF levels by ELISA in the peritoneal lavage from mice. N = 4, Data is analyzed by One-way ANOVA.

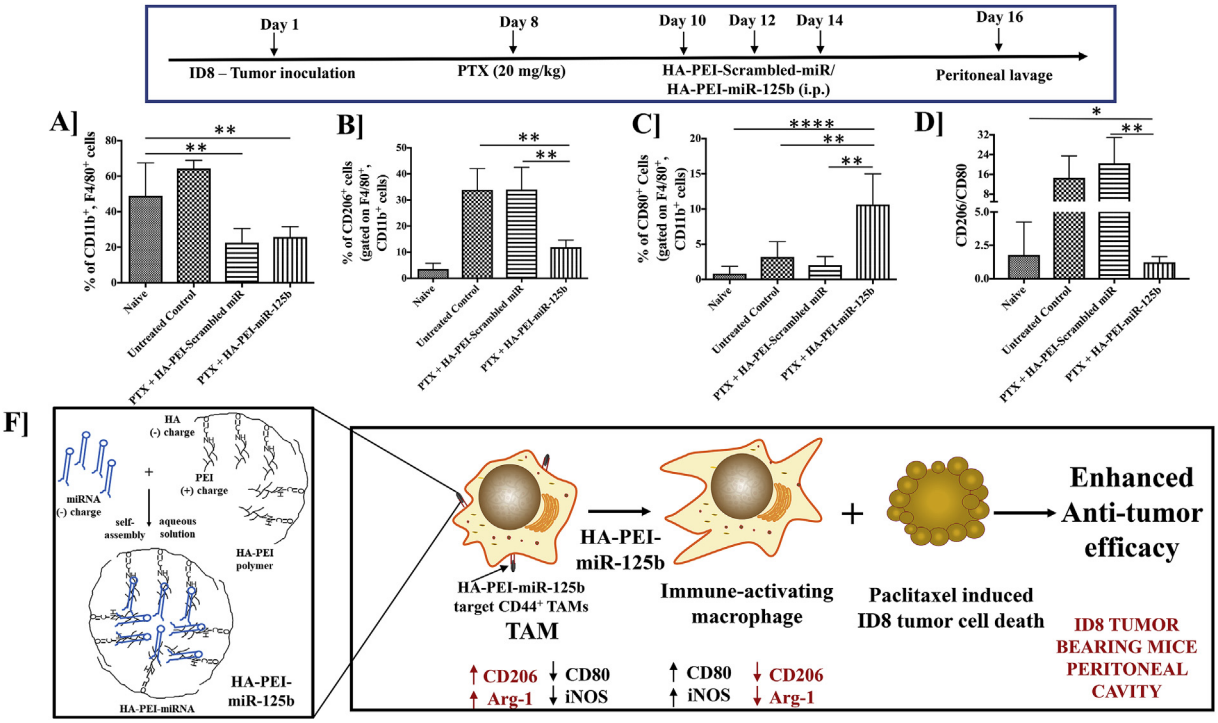

Fig. 6. Analysis of immune cells from the peritoneal lavage fluid upon treatment with combination miR-125b transfection and paclitaxel chemotherapy. Female C57BL/6 mice were injected with ID8 cells on day 1. On day 8th mice were injected intraperitoneally with PTX (2 mg/kg) and on day 10th mice were injected intraperitoneally with either HA-PEI-scrambled miR or HA-PEI-miR-125 b at 1 mg/kg dose every alternate day for 3 days and peritoneal cavity was lavaged with 1X PBS. Peritoneal cells were collected and analysed by FACS for (A) $CD11b^+$, $F4/80^+$ macrophages, (B) $CD206^+$ M2 macrophages and (C) $CD80^+$ M1 macrophages (D) Ratio of $CD206^+/CD80^+$ cells. N = 4, Data is analyzed by One-way ANOVA. (F) Schematic representation of combination therapy with intraperitoneal administration of HA-PEI-miR-125b nanoparticles and paclitaxel as anticancer therapy for epithelial ovarian cancer.

observed ratio of CD206 + /CD80 + cells with the PTX + HA-PEI-miR-125b treatment as compared to untreated control as well as PTX + HA-PEI-scrambled miR (Fig. 6D). Furthermore, there is no difference in the total immune cells ($CD45^+$ cells) (Supplementary Fig. 3A). A significant increase is observed in the PD-1^+ cell population, following treatment with HA-PEI-miR125b nanoparticles in combination with paclitaxel as well as treatment with HA-PEI-scrambled-miR nanoparticles in combination with paclitaxel as compared to the untreated control (Supplementary Fig. 3B). Furthermore, intraperitoneal administration of HA-PEI-miR125b nanoparticles does not induce systemic toxicity as seen in Supplementary Fig. 4.

4. Discussion

The immunocompetent ID8-VEGF syngeneic mouse model of epithelial ovarian cancer closely mimics the progression of human epithelial ovarian cancer along with the characteristic malignant ascites [21,23,24]. Additionally, since VEGF expression is associated with disease progression, ascitic fluid formation, as well as patient survival in epithelial ovarian cancer [25], this ID8 syngeneic mouse model, overexpressing VEGF aptly, simulates advanced stage of the disease [26]. Thus, in this study, we have used VEGF levels in the peritoneal fluid as a marker for tumor progression. Furthermore, ID8-VEGF syngeneic mouse model of epithelial ovarian cancer was well suited for this study since the increase in TAMs in the peritoneal cavity, was well correlated with the markers of tumor progression such as accumulation of ascitic fluid, the presence of peritoneal tumor nodules and VEGF levels in peritoneal fluid (depicted in Fig. 1) [27]. However, it is noted that TAMs express mixed polarization and are represented by various markers among which we have focused on CD206 and CD80 based on our previous study using HA-PEI-miR-125b nanoparticles [21].

We have previously demonstrated the efficiency of intraperitoneal administration of HA-PEI nanoparticles in preferentially targeting the peritoneal macrophages, mediated through the CD44 glycoprotein receptors [28,29]. Additionally, we had screened multiple miRs for their efficiency in TAM repolarization, among which miR-125b showed the highest efficiency [21]. Thus, herein we have used the HA-PEI nanoparticles encapsulating miR-125b having size > 200 nm, PDI < 0.3 and zeta-potential close to -25 mV, making them suitable for uptake by macrophages [30–32]. Following intraperitoneal administration of CY5 labeled HA-PEI nanoparticles in the ID8 ovarian cancer model, the nanoparticles were preferentially taken up by the macrophages. Furthermore, the uptake of Cy5 labeled HA-PEI nanoparticles was highest at 6 h and reduced at 12 h and 24 h due to the efficient time-dependent clearance mechanism of these HA-PEI nanoparticles.

In cases of ovarian cancers restricted to the peritoneal cavity, intraperitoneal administration of paclitaxel and platinum chemotherapy is an approved standard care of treatment [5,33]. Thus, our strategy was to concurrently deliver HA-PEI-miR-125b nanoparticles intraperitoneally for repolarization of TAMs to an immune-activating phenotype for synergistic anti-tumor efficacy in combination therapy with paclitaxel. The total number of $CD11b^+$, $F4/80^+$ macrophages were reduced following intraperitoneal administration of HA-PEI-miR-125b as well as HA-PEI-scrambled miR nanoparticles. Thus, this effect could thus be attributed to the administration of HA-PEI nanoparticles. Since these HA-PEI nanoparticles particularly target macrophages, this could be the immediate effect on the macrophages of the peritoneal cavity. Nevertheless, following intraperitoneal administration of HA-PEI-miR-125b nanoparticles, the significant increase in iNOS levels as compared to HA-PEI-scrambled miR nanoparticles and the significant increase in $CD80^+$ macrophages and reduction in $CD206^+$ macrophages and Arg-1 levels [34–37] as compared to the untreated group showed efficacious repolarization of TAMs to an immune-activating phenotype. Intraperitoneal administration HA-PEI-miR-125b nanoparticles and HA-PEI-scrambled miR enhanced the $CD11b^+$, $CD11c^+$ dendritic cell population as compared to the untreated control group, which could be the non-specific immune activating effect of HA-PEI nanoparticles [38]. Furthermore, TAMs display immunosuppressive mechanisms to promote tumor growth [39]. One of these mechanisms is inhibiting the infiltrating T-cells. Studies have shown that depletion of TAMs, resulted in increase in T-cell infiltration [40]. Thus, similarly repolarization of TAMs to pro-inflammatory phenotype with HA-PEI-miR-125b nanoparticles, could overcome the immunosuppressive tumor environment, thereby promoting infiltrating T-cells. The increase in PD-1^+ immune cells could be the result of increased infiltrating T-cells. However, this hypothesis needs further detailed evaluation. Additionally, no significant difference was observed in the $CD45^+$ immune cells between the untreated control and HA-PEI-miR-125b treated group.

The synergistic anti-tumor efficacy of paclitaxel and HA-PEI-miR-125b was clearly observed with a reduction of ascitic fluid in the peritoneal cavity. Both the paclitaxel with HA-PEI-scrambled miR, PTX alone, HA-PEI-miR125b alone and HA-PEI-miR-125b showed reduced VEGF levels in the peritoneal fluid on day 24 as compared to untreated control group demonstrating paclitaxel alone and HA-PEI-miR125b alone could reduce the VEGF levels. However, there was no significant reduction in VEGF levels with the paclitaxel with HA-PEI-scrambled miR, PTX alone, HA-PEI-miR125b alone and HA-PEI-miR-125b as compared to the untreated control on 16th day. It is known that high-dose of paclitaxel induces stress to the tumor cells and tumor-related endothelium, stimulating VEGF mRNA expression [41,42]. This could be the reason for no change in VEGF levels on day 16th in both the paclitaxel treated groups. However, by day 24th, the cytotoxic activity of paclitaxel results in reduced number of VEGF secreting ID8 cells, in turn significantly reducing the VEGF levels. Additionally, on day 24 the VEGF levels in the PTX with HA-PEI-miR125b treated group was significantly lower than the PTX with HA-PEI-scrambled miR treated group demonstrating the efficient synergistic efficacy of paclitaxel and TAM repolarization. This difference was evident at later time-points indicating that paclitaxel was not efficient in completely eradicating the tumor cells which start proliferating once paclitaxel is cleared [43,44]. Moreover, the presence of TAMs is known to restrict the anti-tumor immune responses associated with chemotherapy [45,46]. Thus, repolarization of TAMs would additionally overcome the limitations imposed by TAMs on anti-tumor immune responses associated with chemotherapy, which would, in turn, enhance the anti-tumor efficacy of the chemotherapeutic agents such as paclitaxel (Fig. 6F). However, treatment of PTX with HA-PEI-miR125b did not significantly reduce VEGF levels compared to PTX alone or PTX with HA-PEI-scrambled miR on day 16, even though HA-PEI-miR125b repolarized TAM towards anti-tumoral phenotype on day 16 since the process of reprogramming/ablation of TAMs to inhibit of tumor growth is a complex with the downstream effects occurring 1–3 weeks post TAM ablation/reprogramming [47–49].

In conclusion, we demonstrate that the intraperitoneal administration of HA-PEI-miR-125b is an effective strategy in specifically targeting TAMs in the peritoneal cavity of the ID8 ovarian tumor model and repolarizing TAMs to immune-activating phenotype. Furthermore, pertaining to the half-live of paclitaxel in the peritoneal cavity, a single dose of paclitaxel can suppress the ID8 ovarian tumors for a limited duration [50,51] while the combination with paclitaxel treatment and TAMs repolarization significantly enhances the anti-tumor efficacy in advanced stages of tumor progression. Importantly, since paclitaxel administered intraperitoneally is the standard care of treatment for ovarian cancers restricted to the peritoneal cavity, HA-PEI-miR-125b nanoparticles can be co-administered for enhanced anti-tumor efficacy. Furthermore, these HA-PEI-miR-125b nanoparticles do not lead to any toxicity and are a safer option as an anticancer therapy for a further clinical evaluation.

Conflict of interest statement

The authors declare that they have conflicts of interest.

Acknowledgments

Financial support for this work was provided by the United States National Cancer Institute of the National Institute of Health through grants R21-CA179652 and R56-CA198492, and the Northeastern University-Dana Farber Cancer Center Joint Program on Cancer Drug Development. We also deeply appreciate the assistance of Dr. Lara Milane with the review of the manuscript and suggestions. Additionally, transmission electron microscopy of the formulations was performed by Mr. William Fowle at the Electron Microscopy Center, Northeastern University (Boston, MA).

Appendix A. Supplementary data

Supplementary data to this article can be found online at https://doi.org/10.1016/j.canlet.2019.07.002.

References

[1] W.A. Cliby, M.A. Powell, N. Al-Hammadi, L. Chen, J. Philip Miller, P.Y. Roland, D.G. Mutch, R.E. Bristow, Ovarian cancer in the United States: contemporary patterns of care associated with improved survival, Gynecol. Oncol. 136 (2015) 11–17.
[2] L.A. Torre, B. Trabert, C.E. DeSantis, K.D. Miller, G. Samimi, C.D. Runowicz, M.M. Gaudet, A. Jemal, R.L. Siegel, Ovarian cancer statistics, 2018, Ca - Cancer J. Clin. 68 (2018) 284–296.
[3] S.A. Cannistra, Cancer of the ovary, N. Engl. J. Med. 351 (2004) 2519–2529.
[4] M. Jose, A. Rauh-Hain, Thomas C. Krivak, Marcela G. del Carmen, Alexander B. Olawaiye, MD2, ovarian cancer screening and early detection in the general population, Rev. Obstet. Gynaecol. 4 (2011).
[5] R.L. Coleman, B.J. Monk, A.K. Sood, T.J. Herzog, Latest research and treatment of advanced-stage epithelial ovarian cancer, Nat. Rev. Clin. Oncol. 10 (2013) 211–224.
[6] S. Narod, Can advanced-stage ovarian cancer be cured? Nat. Rev. Clin. Oncol. (2016) 265.
[7] R.L.C. Bryan T Hennessy, Maurie Markman, Ovarian cancer, Lancet (N. Am. Ed.) (2009) 374.
[8] C. Caux, R.N. Ramos, G.C. Prendergast, N. Bendriss-Vermare, C. Menetrier-Caux, A milestone review on how macrophages affect tumor growth, Cancer Res. 76 (2016) 6439–6442.
[9] A.R. Poh, M. Ernst, Targeting macrophages in cancer: from bench to bedside, Front Oncol 8 (2018) 49.
[10] G. Solinas, G. Germano, A. Mantovani, P. Allavena, Tumor-associated macrophages (TAM) as major players of the cancer-related inflammation, J. Leukoc. Biol. 86 (2009) 1065–1073.
[11] K. Kawamura, Y. Komohara, K. Takaishi, H. Katabuchi, M. Takeya, Detection of M2 macrophages and colony-stimulating factor 1 expression in serous and mucinous ovarian epithelial tumors, Pathol. Int. 59 (2009) 300–305.
[12] M. Heusinkveld, S.H. van der Burg, Identification and manipulation of tumor associated macrophages in human cancers, J. Transl. Med. 9 (2011) 216.
[13] S. Reinartz, T. Schumann, F. Finkernagel, A. Wortmann, J.M. Jansen, W. Meissner, M. Krause, A.M. Schworer, U. Wagner, S. Muller-Brusselbach, R. Muller, Mixed-polarization phenotype of ascites-associated macrophages in human ovarian carcinoma: correlation of CD163 expression, cytokine levels and early relapse, Int. J. Cancer 134 (2014) 32–42.
[14] E. Muller, P.F. Christopoulos, S. Halder, A. Lunde, K. Beraki, M. Speth, I. Oynebraten, A. Corthay, Toll-like receptor ligands and interferon-gamma synergize for induction of antitumor M1 macrophages, Front. Immunol. 8 (2017) 1383.
[15] K.R. Wiehagen, N.M. Girgis, D.H. Yamada, A.A. Smith, S.R. Chan, I.S. Grewal, M. Quigley, R.I. Verona, Combination of CD40 agonism and CSF-1R blockade reconditions tumor-associated macrophages and drives potent antitumor immunity, Cancer Immunol Res 5 (2017) 1109–1121.
[16] S.M. Pyonteck, L. Akkari, A.J. Schuhmacher, R.L. Bowman, L. Sevenich, D.F. Quail, O.C. Olson, M.L. Quick, J.T. Huse, V. Teijeiro, M. Setty, C.S. Leslie, Y. Oei, A. Pedraza, J. Zhang, C.W. Brennan, J.C. Sutton, E.C. Holland, D. Daniel, J.A. Joyce, CSF-1R inhibition alters macrophage polarization and blocks glioma progression, Nat. Med. 19 (2013) 1264–1272.
[17] A. Mantovani, A. Sica, S. Sozzani, P. Allavena, A. Vecchi, M. Locati, The chemokine system in diverse forms of macrophage activation and polarization, Trends Immunol. 25 (2004) 677–686.
[18] S. Zanganeh, G. Hutter, R. Spitler, O. Lenkov, M. Mahmoudi, A. Shaw, J.S. Pajarinen, H. Nejadnik, S. Goodman, M. Moseley, L.M. Coussens, H.E. Daldrup-Link, Iron oxide nanoparticles inhibit tumour growth by inducing pro-inflammatory macrophage polarization in tumour tissues, Nat. Nanotechnol. 11 (2016) 986–994.
[19] T.M. Nywening, A. Wang-Gillam, D.E. Sanford, B.A. Belt, R.Z. Panni, B.M. Cusworth, A.T. Toriola, R.K. Nieman, L.A. Worley, M. Yano, K.J. Fowler, A.C. Lockhart, R. Suresh, B.R. Tan, K.H. Lim, R.C. Fields, S.M. Strasberg, W.G. Hawkins, D.G. DeNardo, S.P. Goedegebuure, D.C. Linehan, Targeting tumour-associated macrophages with CCR2 inhibition in combination with FOLFIRINOX in patients with borderline resectable and locally advanced pancreatic cancer: a single-centre, open-label, dose-finding, non-randomised, phase 1b trial, Lancet Oncol. 17 (2016) 651–662.
[20] A.A. Chaudhuri, A.Y. So, N. Sinha, W.S. Gibson, K.D. Taganov, R.M. O'Connell, D. Baltimore, MicroRNA-125b potentiates macrophage activation, J. Immunol. 187 (2011) 5062–5068.
[21] N.N. Parayath, A. Parikh, M.M. Amiji, Repolarization of tumor-associated macrophages in a genetically engineered nonsmall cell lung cancer model by intraperitoneal administration of hyaluronic acid-based nanoparticles encapsulating MicroRNA-125b, Nano Lett. 18 (2018) (2018) 3571–3579.
[22] A. Mantovani, F. Marchesi, A. Malesci, L. Laghi, P. Allavena, Tumour-associated macrophages as treatment targets in oncology, Nat. Rev. Clin. Oncol. 14 (2017) 399–416.
[23] C.C.T. Katherine, F. Roby, Jeffrey P. Sweetwood, Ying Cheng, Judith L. Pace, Ossama Tawfik, Diane L. Persons, Peter G. Smith, Paul F. Terranova, Development of a syngeneic mouse model for events related to ovarian cancer, Carcinogenesis 21 (April) (2000) 585–591.
[24] Y.S. Sungpil Cho, Andrew P. Soisson, Mark K. Dodson, C. Matthew Peterson, Elke A. Jarboe, Anne M. Kennedy, Margit M. Janat-Amsbury, Characterization and evaluation of pre-clinical suitability of a syngeneic orthotopic mouse ovarian cancer model, Anticancer Res. 33 (2013) 1317–1324.
[25] A.J. Cortez, P. Tudrej, K.A. Kujawa, K.M. Lisowska, Advances in ovarian cancer therapy, Cancer Chemother. Pharmacol. 81 (2018) 17–38.
[26] M.M. Janat-Amsbury, J.W. Yockman, M.L. Anderson, D.G. Kieback, S.W. Kim, Comparison of ID8 MOSE and VEGF-modified ID8 cell lines in an immunocompetent animal model for human ovarian cancer, Anticancer Res. 26 (2006) 2785–2789.
[27] M. Yin, X. Li, S. Tan, H.J. Zhou, W. Ji, S. Bellone, X. Xu, H. Zhang, A.D. Santin, G. Lou, Tumor-associated macrophages drive spheroid formation during early transcoelomic metastasis of ovarian cancer, J. Clin. Investig. 126 (2016) 4157–4173.
[28] I.A. Ganesh S, D.V. Morrissey, M.M. Amiji, Hyaluronic acid based self-assembling nanosystems for CD44 target mediated siRNA delivery to solid tumors, Biomaterials 34 (2013) 3489–3502.
[29] R.R. Thanh-Huyen Tran, Juili Shelke, Mansoor M. Amiji, Modulation of macrophage functional polarity towards anti-inflammatory phenotype with plasmid DNA delivery in CD44 targeting hyaluronic acid nanoparticles, Sci. Rep. 5 (2015).
[30] N. Oh, J.H. Park, Endocytosis and exocytosis of nanoparticles in mammalian cells, Int. J. Nanomed. 9 (Suppl 1) (2014) 51–63.
[31] L. Shang, K. Nienhaus, G.U. Nienhaus, Engineered nanoparticles interacting with cells: size matters, J. Nanobiotechnol. 12 (2014) 5.
[32] D.S. Spencer, A.S. Puranik, N.A. Peppas, Intelligent nanoparticles for advanced Drug delivery in cancer treatment, Curr Opin Chem Eng 7 (2015) 84–92.
[33] M. Markman, J.L. Walker, Intraperitoneal chemotherapy of ovarian cancer: a review, with a focus on practical aspects of treatment, J. Clin. Oncol. 24 (2006) 988–994.
[34] V. Briken, D.M. Mosser, Editorial: switching on arginase in M2 macrophages, J. Leukoc. Biol. 90 (2011) 839–841.
[35] A. Mantovani, S. Sozzani, M. Locati, P. Allavena, A. Sica, Macrophage polarization: tumor-associated macrophages as a paradigm for polarized M2 mononuclear phagocytes, Trends Immunol. 23 (2002) 549–555.
[36] W. Ying, P.S. Cheruku, F.W. Bazer, S.H. Safe, B. Zhou, Investigation of macrophage polarization using bone marrow derived macrophages, J. Vis. Exp. 76 (2013) e50323.
[37] M. Jaguin, N. Houlbert, O. Fardel, V. Lecureur, Polarization profiles of human M-CSF-generated macrophages and comparison of M1-markers in classically activated macrophages from GM-CSF and M-CSF origin, Cell. Immunol. 281 (2013) 51–61.
[38] F. Zamboni, S. Vieira, R.L. Reis, J.M. Oliveira, M.N. Collins, The potential of hyaluronic acid in immunoprotection and immunomodulation: chemistry, processing and function, Prog. Mater. Sci. 97 (2018) 97–122.
[39] Y. Komohara, Y. Fujiwara, K. Ohnishi, M. Takeya, Tumor-associated macrophages: potential therapeutic targets for anti-cancer therapy, Adv. Drug Deliv. Rev. 99 (2016) 180–185.
[40] C. Caux, R.N. Ramos, G.C. Prendergast, N. Bendriss-Vermare, C. Ménétrier-Caux, A milestone review on how macrophages affect tumor growth, Cancer Res. 76 (2016) 6439–6442.
[41] H.S. Kim, J.M. Oh, D.H. Jin, K.-H. Yang, E.-Y. Moon, Paclitaxel induces vascular endothelial growth factor expression through reactive oxygen species production, Pharmacology 81 (2008) 317–324.
[42] E.-K. Choi, S.-W. Kim, E.-J. Nam, J. Paek, G.-W. Yim, M.-H. Kang, Y.-T. Kim, Differential effect of intraperitoneal albendazole and paclitaxel on ascites formation and expression of vascular endothelial growth factor in ovarian cancer cell-bearing athymic nude mice, Reprod. Sci. 18 (2011) 763–771.
[43] F. Mohamed, P. Marchettini, O.A. Stuart, P.H. Sugarbaker, Pharmacokinetics and tissue distribution of intraperitoneal paclitaxel with different carrier solutions, Cancer Chemother. Pharmacol. 52 (2003) 405–410.
[44] M. Tsai, Z. Lu, J. Wang, T.K. Yeh, M.G. Wientjes, J.L. Au, Effects of carrier on disposition and antitumor activity of intraperitoneal Paclitaxel, Pharm. Res. (N. Y.) 24 (2007) 1691–1701.
[45] M. De Palma, C.E. Lewis, Cancer: macrophages limit chemotherapy, Nature 472 (2011) 303–304.
[46] D.G. DeNardo, D.J. Brennan, E. Rexhepaj, B. Ruffell, S.L. Shiao, S.F. Madden,

W.M. Gallagher, N. Wadhwani, S.D. Keil, S.A. Junaid, H.S. Rugo, E.S. Hwang, K. Jirstrom, B.L. West, L.M. Coussens, Leukocyte complexity predicts breast cancer survival and functionally regulates response to chemotherapy, Cancer Discov. 1 (2011) 54–67.

[47] T.M. Robinson-Smith, I. Isaacsohn, C.A. Mercer, M. Zhou, N. Van Rooijen, N. Husseinzadeh, M.M. McFarland-Mancini, A.F. Drew, Macrophages mediate inflammation-enhanced metastasis of ovarian tumors in mice, Cancer Res. 67 (2007) 5708–5716.

[48] N.R. Miselis, Z.J. Wu, N. Van Rooijen, A.B. Kane, Targeting tumor-associated macrophages in an orthotopic murine model of diffuse malignant mesothelioma, Mol. Cancer Ther. 7 (2008) 788–799.

[49] H. Fujimoto, T. Sangai, G. Ishii, A. Ikehara, T. Nagashima, M. Miyazaki, A. Ochiai, Stromal MCP-1 in mammary tumors induces tumor-associated macrophage infiltration and contributes to tumor progression, Int. J. Cancer 125 (2009) 1276–1284.

[50] F. Innocenti, R. Danesi, A. Di Paolo, C. Agen, D. Nardini, G. Bocci, M. Del Tacca, Plasma and tissue disposition of paclitaxel (taxol) after intraperitoneal administration in mice, Drug Metab. Dispos. 23 (1995) 713–717.

[51] B. Sun, M.S. Taha, B. Ramsey, S. Torregrosa-Allen, B.D. Elzey, Y. Yeo, Intraperitoneal chemotherapy of ovarian cancer by hydrogel depot of paclitaxel nanocrystals, J. Control. Release 235 (2016) 91–98.